

Field dependence of the vortex core size

V. G. Kogan and N. V. Zhelezina

Ames Laboratory-DOE and Department of Physics and Astronomy, Iowa State University, Ames, Iowa 50011-3160, USA

(Received 26 July 2004; revised manuscript received 28 January 2005; published 13 April 2005)

We show that the field dependence of the coherence length $\xi(H)$ calculated within the weak-coupling BCS theory for clean superconductors at low temperatures and high fields is qualitatively the same as the H dependence of the vortex core size ρ_c recorded experimentally in a number of superconductors with high Ginzburg-Landau parameter κ . We argue that H dependencies of ξ and ρ_c are weakened by scattering and temperature and disappear in the dirty limit and as $T \rightarrow T_c$. We find that the high-field slope $d\rho_c/d(H^{-1/2})$ for clean materials at low T 's is nearly material independent, and we provide an estimate of this nearly universal slope, the prediction supported by the data available.

DOI: 10.1103/PhysRevB.71.134505

PACS number(s): 74.20.-z, 74.25.-q, 74.25.Op

I. INTRODUCTION

The coherence length ξ has first been introduced as a phenomenological length scale in the near- T_c Ginzburg-Landau (GL) description where it sets, among other things, the “vortex core size” ρ_c . Since the core, in fact, does not have a sharp boundary, the size ρ_c cannot be unambiguously defined and is commonly chosen “operationally convenient,” i.e., in a way that varies from one experimental or theoretical situation to another. For example, ρ_c may be defined as the radius of a circle where the persistent current is maximum,¹ or—within the London approach—as the distance at which the divergent London current density reaches the depairing value, or assuming the core being a normal cylinder and equating the core contribution to the vortex energy to $(H_c^2/8\pi)\pi\rho_c^2$ with $H_c^2/8\pi$ being the condensation energy.^{2,3} Another example comes from the scanning tunneling work where “the vortex core radius is arbitrary defined by that distance ρ_c from the vortex center for which the tunneling current has decreased from I_{\max} to 36% of $I_{\max} - I_{\min}$.”⁴ Clearly, these procedures yield different values of ρ_c , although all of them have the same order of magnitude.

A lot of experimental effort has been invested recently in the study of the vortex core size; see the review by Sonier and references therein.¹ Notably, whatever the definition of ρ_c is adopted, the low temperature ρ_c is shown to decrease with increasing field in a number of materials, such as NbSe₂, V₃Si, LuNi₂B₂C, YBa₂Cu₃O_{7- δ} , and CeRu₂, physical characteristics of which have little to do with each other (except all of them have a large GL parameter $\kappa = \lambda_L/\xi$). The dependences $\rho_c(H)$ for all tested materials are qualitatively similar; for large fields $\rho_c \sim 1/\sqrt{H}$. Properties of the quasi-particle spectrum inside and outside the cores (where the excitations may form narrow conducting bands) are considered responsible for the H and T dependences of ρ_c .

In this paper we study the relation between experimentally determined ρ_c and the coherence length ξ calculated within the weak-coupling BCS theory for arbitrary T and H . We argue that near the vortex centers where the order parameter $\Delta \rightarrow 0$ and the field is practically uniform for large κ 's, one can use for determination of ξ the same formal procedure as that employed in the seminal work of Helfand and

Werthamer (HW) on the upper critical field $H_{c2}(T)$, the situation in which $\Delta \rightarrow 0$ and the field is uniform. This yields the field dependence of ξ , which agrees qualitatively with observed $\rho_c(H)$.

A few examples of numerical solutions of the microscopic equations of superconductivity show that the H dependence of ρ_c follows from the theory under very general assumptions.⁶⁻⁸ Our approach can be applied to the problem of $\rho_c(H)$ only in large fields of high- κ materials; still, we obtain our main results analytically, which has certain advantages as compared to however powerful numerical techniques, and enables one to make experimentally verifiable predictions. For example, we show that the H dependence of ρ_c is weakened by scattering and disappears in the dirty limit; also it vanishes as $T \rightarrow T_c$. Besides, $\xi(H)$ is weakly affected by peculiarities of the Fermi surface, i.e., we expect qualitatively the same dependence at low temperatures for various clean materials, the high-field slope $d\rho_c/d(H^{-1/2})$ is nearly universal.

We begin with the notion that within the microscopic theory, at arbitrary magnetic fields H and temperatures T , it is not clear what exact value one should assign to ξ . The difficulty comes from the fact that ξ is not among the basic input parameters of the theory; instead, it should be calculated, in general a very difficult if at all possible analytic task. There is, however, a region at the second-order phase transition from superconducting to normal state, the SN boundary, where the theory can be linearized and, consequently, ξ is well defined.

The linearization has been performed by HW in the work of on the upper critical field $H_{c2}(T, \tau)$ with τ being the mean scattering time on nonmagnetic impurities.⁵ They have shown that at H_{c2} , where the order parameter Δ goes to zero, it satisfies for any T a linear equation,

$$-\xi^2(T)\Pi^2\Delta = \Delta, \quad (1)$$

where $\Pi = \nabla + 2\pi i\mathbf{A}/\phi_0$ is the gauge-invariant gradient, \mathbf{A} is the vector potential, and ϕ_0 is the flux quantum. Formally, the equation is equivalent to the Schrödinger equation for a charge in uniform magnetic field; the field H_{c2} at which superconductivity first nucleates in a bulk sample corresponds

to the lowest eigenvalue of this equation, $H_{c2} = \phi_0 / 2\pi\xi^2$. This field (and ξ) is obtained by solving the basic self-consistency equation of the theory

$$\frac{\hbar}{2\pi T} \ln \frac{T_c}{T} = \sum_{\omega=0}^{\infty} \left(\frac{1}{\omega} - \frac{2\tau S}{\beta - S} \right), \quad (2)$$

where the function $S(T, \xi, \tau)$ can be written as

$$S = \frac{2\beta}{\ell q} \int_0^{\infty} ds e^{-s^2} \tan^{-1} \frac{s\ell q}{\beta} \quad (3)$$

$$= \sum_{j=0}^{\infty} \frac{j!}{2j+1} \left(-\frac{\ell^2 q^2}{\beta^2} \right)^j, \quad (4)$$

$$\beta = 1 + 2\omega\tau, \quad q^2 = 2\pi H_{c2} / \phi_0 = \xi^{-2}. \quad (5)$$

Here, $\omega = \pi T(2n+1)/\hbar$, n is an integer, v is the Fermi velocity, and $\ell = v\tau$ is the mean-free path. The power-series representation of S is obtained by formally expanding \tan^{-1} and then integrating over s . The evaluation of S was performed for the isotropic Fermi surface, i.e., for a Fermi sphere.

Thus, strictly speaking, the length ξ is defined only at the SN phase boundary $H_{c2}(T)$, and the question remains whether or not the same definition of ξ is useful out of the immediate vicinity of $H_{c2}(T)$. In fact, in a variety of situations (small samples, proximity systems) the SN transition may take place far from the bulk $H_{c2}(T)$. To approach the problem of the phase boundary in these systems, one has to know $\xi(H, T)$ in a broad domain of the H - T plane away of the bulk $H_{c2}(T)$.

A method to evaluate $\xi(H, T)$ had been developed in Refs. 9 and 10. In principle, the method follows HW by utilizing the field *uniformity* and the Δ *smallness* at the SN transition, wherever it occurs. Below, we outline the method as applied to the three-dimensional (3D) isotropic case of a Fermi sphere. Then, we consider two-dimensional (2D) isotropic materials, i.e., the Fermi cylinder. We find that away from the critical temperature T_c of clean superconductors, $\xi(H, T)$ so obtained *decreases* when H *increases* toward H_{c2} ; the effect is suppressed by impurity scattering and is absent in the dirty limit. We provide a closed-form equation for $\xi(H)$ for the zero- T clean case for both Fermi sphere and cylinder and show that the results can be represented as

$$\frac{\xi(H)}{\xi(H_{c2})} = U \left(\frac{H}{H_{c2}} \right) \quad (6)$$

with U being an universal function.

We next argue that the same procedure can be applied to the mixed state in applied fields $H < H_{c2}$ near the vortex core centers in materials with large $\kappa = \lambda_L / \xi$. This is because near the centers $\Delta(r) \rightarrow 0$ and the field (varying on the scale of the London penetration depth λ_L) can be taken as *uniform*. We find our results on $\xi(H)$ in qualitative agreement with the data available on $\rho_c(H)$, uncertainties of experimental procedures of extracting ρ_c notwithstanding.

II. FERMI SPHERE: $H_{c2}(T)$ AND $S(H, \xi, \omega, \ell)$

Here we reproduce major points of the $\xi(H)$ derivation for the system near the second-order SN transition with the help of the quasiclassical Eilenberger formalism.¹¹ The main equations of the theory read

$$\boldsymbol{\tau v} \cdot \boldsymbol{\Pi} f = g(F + 2\tau\Delta) - (G + 2\omega\tau)f, \quad (7)$$

$$\frac{\Delta}{2\pi T} \ln \frac{T_c}{T} = \sum_{\omega=0}^{\infty} \left(\frac{\Delta}{\hbar\omega} - F \right). \quad (8)$$

Here, \mathbf{v} is the Fermi velocity; $f(\mathbf{r}, \omega, \mathbf{v})$ and $g(\mathbf{r}, \omega, \mathbf{v})$ are the Eilenberger Green's functions with averages over the Fermi surface, denoted as $F = \langle f \rangle$ and $G = \langle g \rangle$.

In the normal phase $f=0$ and $g=1$. In a small vicinity of the SN transition, $|f| \ll 1$, whereas g can still be set unity in linear approximation in f due to normalization $g = (1 - ff^\dagger)^{1/2}$ (for the same reason we do not need here an equation for f^\dagger). Equation (7) can be linearized

$$\ell \cdot \boldsymbol{\Pi} f = \tilde{F} - \beta f, \quad (9)$$

$$\ell = \mathbf{v}\tau, \quad \tilde{F} = F + 2\tau\Delta/\hbar, \quad \beta = 1 + 2\omega\tau. \quad (10)$$

The solution of Eq. (9) is written as

$$f = (\beta + \ell \cdot \boldsymbol{\Pi})^{-1} \tilde{F} = \int_0^{\infty} d\rho e^{-\rho(\beta + \ell \cdot \boldsymbol{\Pi})} \tilde{F}, \quad (11)$$

or for the Fermi surface average

$$F = \int_0^{\infty} d\rho e^{-\rho\beta} \langle e^{-\rho\ell \cdot \boldsymbol{\Pi}} \tilde{F} \rangle. \quad (12)$$

We now assume that Δ , F , and \tilde{F} satisfy Eq. (1); then, utilizing commutators of the operator $\boldsymbol{\Pi}$ in a uniform field and the known properties of exponential operators,⁹ one can manipulate Eq. (12) to

$$F(\mathbf{r}, \omega) = \Delta(\mathbf{r}) \frac{2\tau S}{\beta - S}, \quad (13)$$

where

$$S = \sum_{m,j=0}^{\infty} \frac{(-q^2)^j}{j!(2m+2j+1)} \left[\frac{(m+j)!}{m!} \right]^2 \left(\frac{\ell^2}{\beta^2} \right)^{m+j} \times \prod_{i=1}^m [(2i-1)q^2 - \xi^{-2}], \quad q^2 = \frac{2\pi H}{\phi_0}. \quad (14)$$

After substituting F of Eq. (13) in the self-consistency Eq. (8) and canceling $\Delta(\mathbf{r})$, we obtain an implicit Eq. (2) for $\xi(H, T, \ell)$. It is easy to see that at the bulk H_{c2} where $q^2 = 1/\xi^2$, the series (14) reduces to the HW sum (4).

The double sum (14) is, in fact, an asymptotic series and is difficult to deal with when the goal is to solve Eq. (2) for $\xi(H, T, \ell)$. The situation simplifies greatly in the dirty limit: S is an expansion in powers of ℓ . Keeping only the terms with $m+j=0, 1$, one obtains

$$S = 1 - \frac{\ell^2}{3\xi^2\beta^2}, \quad \ell^4/\xi^4 \ll 1, \quad \ell^4q^4 \ll 1. \quad (15)$$

When substituted in the self-consistency Eq. (2), this yields a de Gennes-Maki dirty-limit result for $\xi(T, \ell)$ and $H_{c2}(T)$.² Since the field q^2 does not enter S , *the coherence length in the dirty limit is field independent*. In other words, in the dirty limit, the coherence length at a given T determined at the bulk upper critical field, is the same at this T for any H .

Formally similar situation takes place near the critical temperature T_c where the truncation (15) is justified by smallness of q^2 and ξ^{-2} (not of ℓ). We conclude that *near T_c the coherence length is field independent for any ℓ* . We then expect the strongest H dependence of ξ to exist at low temperatures in clean materials.

Given the complexity of series (14), it is desirable to have an integral representation for S better suited for analytic and numerical work. This had been done in Ref. 10 for the 3D case of a spherical Fermi surface. We refer the reader for details of this nontrivial procedure and provide here the result (a similar procedure for the 2D case is described in Sec. III and Appendix B)

$$S(u, \sigma) = \sqrt{\pi} \operatorname{Re} \int_0^\infty ds \frac{(1-us^2)^{\sigma-1}}{(1+us^2)^\sigma} \operatorname{erfc} s, \quad (16)$$

$$u = \frac{\ell^2 q^2}{\beta^2}, \quad \sigma = \frac{1}{2} \left(1 + \frac{1}{\xi^2 q^2} \right); \quad (17)$$

$\operatorname{erfc} s = (2/\sqrt{\pi}) \int_s^\infty dz \exp(-z^2)$ (σ here differs by the sign from that used in Ref. 10). Note that $\sigma=1$ at H_{c2} ; integration by parts in (16) gives the HW integral (3). One can check by formally expanding the integrand in powers of us^2 and integrating over s that the integral (16) can indeed be written as the series (14) (see Appendix B in Ref. 10). A similar expansion for the 2D case is given in Sec. III.

III. FERMI CYLINDER

The calculations of the previous section cannot be done for an arbitrary Fermi surface. Still, for some simple shapes it is possible. The simplest of those is the Fermi cylinder with the field parallel to the cylinder axis. Employing the same procedure outlined for the Fermi sphere, we arrive at

$$S = \sum_{m,n=0}^{\infty} \frac{(-1)^n 2^m (2m+2n)!}{n!(m!)^2} \left(\frac{u}{4} \right)^{m+n} (1-\sigma)_m, \quad (18)$$

where u and σ are defined in Eq. (17); we use the notation $(1-\sigma)_m = (1-\sigma)(2-\sigma)\dots(m-\sigma)$.¹² The integral representation of this sum can be obtained in a manner similar to that described in Ref. 10 for the 3D case,

$$S(u, \sigma) = \frac{2}{\sqrt{\pi}} \operatorname{Re} \int_0^\infty ds \frac{(1-us^2)^{\sigma-1}}{(1+us^2)^\sigma} e^{-s^2} \quad (19)$$

(see Appendix A). To verify this result we write

$$\begin{aligned} \frac{(1-s^2u)^{\sigma-1}}{(1+s^2u)^\sigma} &= \left(\frac{1-s^2u}{1+s^2u} \right)^{\sigma-1} \frac{1}{1+s^2u} \\ &= \sum_m \binom{\sigma-1}{m} \left(-\frac{2us^2}{1+us^2} \right)^m \frac{1}{1+s^2u} \\ &= \sum_{m,n} \frac{(-1)^\mu \mu! (\sigma-1)_m}{(m!)^2 n!} 2^m u^\mu s^{2\mu}, \end{aligned} \quad (20)$$

where $\mu=m+n$. Substituting this into Eq. (19) and integrating over s one obtains S in the form (18).

Having the quantity $S(H, \xi, \omega, \ell)$ for both 3D (Fermi sphere) and 2D (Fermi cylinder), one can solve Eq. (2) for $\xi(H, T, \ell)$ that, in general, can be done numerically. As pointed out above, the most interesting is the situation at $T=0$ in clean materials; this case can be treated analytically.

IV. CLEAN MATERIALS AT $T=0$

To deal with the divergence of $\ln(T_c/T)$ in Eq. (2) we note that the sum over ω on the right-hand side is actually extended to the Debye frequency ω_D . Then, we have for the finite sum

$$\sum_{\omega>0}^{\omega_D} \frac{1}{\hbar\omega} \approx \frac{1}{2\pi T} \ln \frac{2\hbar\omega_D e^\gamma}{\pi T}, \quad (21)$$

where the neglected terms are of the order $T^2/\hbar^2\omega_D^2$ and $\gamma \approx 0.577$ is the Euler constant. Hence the divergent $\ln T$ in Eq. (2) drops off. Since in the clean limit $\beta \approx 2\omega\tau$ and $2\pi S/(\beta - S) \approx S/\omega$ we obtain instead of Eq. (2) in the zero- T limit

$$\ln \frac{2\hbar\omega_D}{\Delta_0} = 2\pi T \sum_{\omega>0}^{\omega_D} \frac{S}{\hbar\omega} \rightarrow \int_0^{\omega_D} \frac{d\omega}{\omega} S(u, \sigma). \quad (22)$$

The integral at the right-hand side diverges logarithmically with increasing ω_D , and so does the left-hand side; in other words, ω_D should drop off the result. This integral is evaluated in Appendix B for both 3D and 2D cases.

As a result we obtain an implicit equation for ξ

$$\ln \frac{\hbar v q}{\Delta_0 \alpha} + \frac{\cos(\pi\sigma)}{4} \left[\psi \left(\frac{1+\sigma}{2} \right) - \psi \left(\frac{\sigma}{2} \right) \right] + \frac{\psi(\sigma)}{2} = 0, \quad (23)$$

where ψ is the Digamma function. The only difference between the 2D and 3D situations is in the number α

$$\alpha_{2D} = \sqrt{2}, \quad \alpha_{3D} = e/\sqrt{2}. \quad (24)$$

Setting $\sigma=1$ in Eq. (23) one obtains

$$H_{c2} = \frac{\phi_0}{2\pi\xi_{c2}^2}, \quad \xi_{c2} = \frac{\hbar v}{\Delta_0 \sqrt{2\alpha}} e^{-\gamma/2}. \quad (25)$$

This yields for the 3D case

$$H_{c2}(0) = \frac{\phi_0 \Delta_0^2}{2\pi \hbar^2 v^2} e^{2+\gamma}, \quad (26)$$

the value obtained variationally by Gor'kov¹³ and proven to be exact by HW; in HW-reduced units it corresponds to $h^*(0) = H_{c2}(0)/T_c H'_{c2}(T_c) \approx 0.72$.⁵ For the 2D case, this gives $h^*(0) \approx 0.59$, the result obtained by Bulaevskii.¹⁴

We now observe that material parameters enter Eq. (23) only in the first term under the log sign. If one measures the length in units of ξ_{c2} and uses the reduced field $h = H/H_{c2}$, then Eq. (23) takes the form independent of material parameters

$$\ln(2he^\gamma) + \frac{\cos(\pi\sigma)}{2} \left[\psi\left(\frac{1+\sigma}{2}\right) - \psi\left(\frac{\sigma}{2}\right) \right] + \psi(\sigma) = 0, \quad (27)$$

$$\sigma = \frac{1}{2} \left(\frac{1}{h\xi^{*2}} + 1 \right), \quad \xi^* = \frac{\xi}{\xi_{c2}}.$$

Hence, this equation defines a universal curve $\xi^*(h)$ independent of either material characteristics v_F, Δ_0 or the dimensionality. Given this curve and $H_{c2}(0)$, one can recover $\xi(H)$ for a clean material at $T=0$.

The curve $\xi(H)/\xi(H_{c2}) = U(H/H_{c2})$ is shown as a solid line in Fig. 1 for $0.15 < H/H_{c2} < 1$; the reason why the small fields domain is not shown is given in Sec. V. Also shown are results of numerical evaluation of $\xi(H)$ for a few values of the impurity parameter $\lambda = \hbar v / 2\pi T_c \ell$. The numerical calculation is done with the help of the self-consistency Eq. (2) for arbitrary T and λ ; $S(\xi, q^2, \omega, \lambda)$ is evaluated using an explicitly real form given in Appendix C.

It is worth noting that the effect of raising temperature on $\xi(H)$ is qualitatively similar to that of the impurity scattering (see solid dots for $t = T/T_c = 0.5$); both suppress the field dependence of ξ . However, at low temperatures for reasonably clean materials in a broad domain of high fields, $\xi(H)$ is well represented by the zero- T clean-limit curve; it is seen in Fig. 1(a) that for $\lambda = 0.25$ this domain extends down to $h \approx 0.4$.

Figure 1(b) shows the same results plotted against $1/\sqrt{h}$, the quantity proportional to the intervortex spacing. In this manner the data are often presented to examine possible connection between the field dependence of the core size $\rho_c(H)$ and other properties of the mixed state.¹ Our result shows that for materials on the clean side with $\lambda < 1$, the slope $d\xi^*/d(h^{-1/2})$ for $H \rightarrow H_{c2}$ is universal. In fact, using Eq. (27) this slope at H_{c2} can be evaluated for the clean limit at $T=0$

$$\left. \frac{d\xi^*}{d(h^{-1/2})} \right|_{h=1} = 1 - \frac{8}{\pi^2} \approx 0.189. \quad (28)$$

We also observe that for real materials with $\lambda \neq 0$ and $T \neq 0$, $\xi^*(h)$ becomes flat as the field decreases with the impurity and temperature-dependent plateaus.

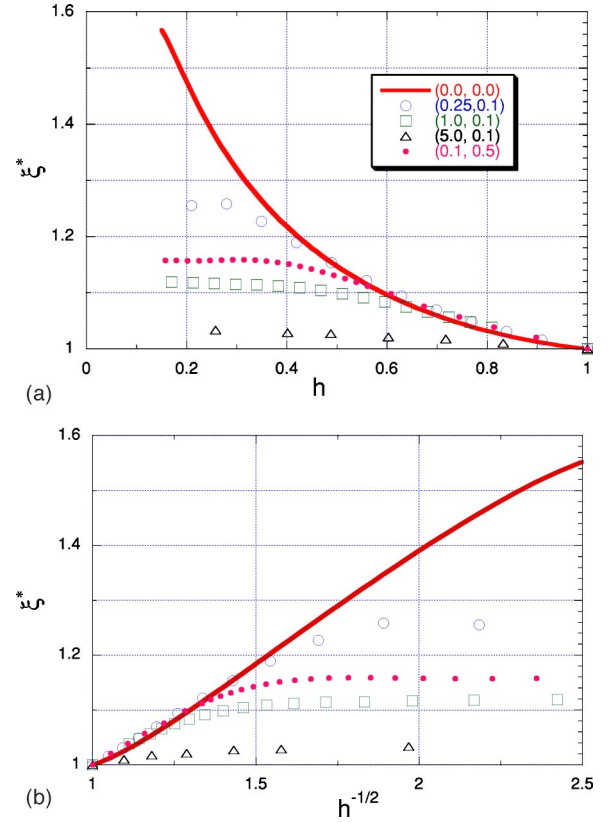


FIG. 1. (Color online) (a) the normalized coherence length $\xi^* = \xi(H)/\xi(H_{c2})$ vs $h = H/H_{c2}$. The solid line is calculated with the help of Eq. (27) for the clean limit at $T=0$. The open symbols show $\xi^*(\lambda, t, h)$ for a few values of the scattering parameter $\lambda = \hbar v / 2\pi T_c \ell$ and reduced temperatures $t = 0.1$ shown in pairs (λ, t) on the legend. The full symbols are for a clean material at an elevated temperature: $(\lambda, t) = (0.1, 0.5)$. (b) ξ^* vs $1/\sqrt{h}$.

V. CORE SIZE

The above discussion of $\xi(H)$ applies at the SN second-order phase transition where the field is uniform and the order parameter Δ goes to zero. In fact, these conditions are met in vortex cores of high- κ type-II superconductors in high fields. Indeed, in this case the field within the core of a size ξ is practically uniform since it varies on a much larger scale λ_L . Besides, when one approaches the vortex center, $\Delta \rightarrow 0$. To evaluate ξ in this situation, one can use the same formalism as at the SN phase boundary; in other words, the above procedure of evaluating $\xi(H)$ can be used to characterize the size ρ_c . In particular, the properties established for $\xi(H)$ should pertain also to $\rho_c(H)$. The most important features of the H dependence of ξ are as follows: (i) this dependence is weakened by scattering and disappears in the dirty limit; (ii) the H dependence of ξ vanishes as $T \rightarrow T_c$; (iii) $\xi(H)$ is weakly affected by peculiarities of the Fermi surface (i.e., we expect qualitatively the same dependence for various materials); (iv) in reduced variables, the dimensionless coherence length $\xi^* = \xi/\xi_{c2}$ should be nearly universal function of the reduced field $h = H/H_{c2}$ for clean materials in high fields and low temperatures; and (v) for materials on the clean side ($\lambda < 1$) the low- T slope $d\xi^*/d(h^{-1/2})$ is nearly universal in

high fields ($h \rightarrow 1$), but ξ becomes H independent in decreasing fields. These features translated to the properties of the core size can be checked experimentally.

One should put a note of caution on our claim of “universality.” This feature expressed in Eq. (27), has been derived for two simple Fermi surfaces, a sphere and a cylinder.¹⁵ Nevertheless, since the Fermi surface shape always enters calculations of macroscopic parameters as ξ or λ_L via averaging over the whole surface, one does not expect the fine features of the surface to drastically alter our conclusion (except in special circumstances, e.g., when the local density of states has sharp maxima at the surface). With this caveat we will use the term “universality” in further discussion.

There is another drawback to our approach. When applied to the SN phase boundary, say, of a proximity sandwich, the field H in the $\xi(H)$ dependence is the externally controlled uniform applied field H_a . Relating here the core size to $\xi(H)$, we imply that H is the field value at the vortex center H_0 , which is nearly constant within the core provided $\kappa \gg 1$. However, the difficulty is that no reliable and generally applicable estimate of H_0 in terms of H_a is available, except numerical results with a particular choice of parameters for low- κ and for high- T_c materials.^{6–8} Another exception is the case of isolated vortices in the GL domain, where $H_0 \approx 2H_{c1}$.¹⁶ In a more interesting situation of $H_a \gg H_{c1}$, the vortex fields are strongly overlapped and variations of the actual field within the vortex lattice are weak relative to the applied field; in fact, they are on the order of $H_{c1} \ll H_a$. Here an error made by considering the field at the vortex axes as equal to the applied field is small. In other words, relating the vortex core size $\rho_c(H_a)$ to $\xi(H_a)$ has a reasonable chance of success only in large fields $H_a \gg H_{c1}$ and improves as $H_a \rightarrow H_{c2}$.

There is also a formal difficulty we encounter attempting to extend the analysis to low fields. In fact, the curve shown in Fig. 1 and generated by solving Eq. (27) shows oscillating behavior if extended to fields below $h \approx 0.15$.¹⁷ Our numerical work for finite λ and T shows that these oscillations are washed out quickly with increasing scattering and/or temperature and are hardly seen for $\lambda > 0.25$ (i.e., in still rather clean materials).

VI. COMPARISON WITH DATA

Relating the results obtained to information available on the vortex core size, we focus on the μ SR data reviewed recently by Sonier.¹ This technique allows one to obtain the field distribution $h(\mathbf{r})$ within the vortex lattice. Then one can calculate the current distribution and define the core radius ρ_c as the distance from the vortex axis to the current maximum in the nearest neighbor direction. This definition of the core size is independent of a model one may choose to theoretically describe the distribution $h(\mathbf{r})$, the point stressed in Ref. 18. We will consider here the data on so defined ρ_c .

The μ SR data on $h(\mathbf{r})$ can also be analyzed with the help of the London model or its nonlocal version. For simplicity, we consider here the standard London isotropic result

$$h(\mathbf{r}) = B \sum_{\mathbf{G}} \frac{e^{i\mathbf{G}\cdot\mathbf{r}}}{1 + \lambda_L^2 G^2}, \quad (29)$$

where B is the magnetic induction and the sum is extended over the reciprocal lattice \mathbf{G} .

It is relevant for this discussion that (a) the London model contains only one length scale, the penetration depth λ_L , and (b) the model implies the constant order parameter Δ and therefore breaks down at distances of the order ξ . The latter comes about formally in Eq. (29) since the sum is divergent (this is readily seen as the logarithmic divergence of h when $r \rightarrow 0$). To mend this inherent shortcoming of the London model, various cutoffs are commonly used, e.g., by introducing a factor $\exp(-\text{const } G^2 \xi^2)$, which excludes distances smaller than ξ . Numerous efforts to fix the constant’s value notwithstanding (see, e.g., Ref. 19), in practice this constant is used quite liberally depending on the application in question. Other cutoffs basically suffer of similar uncertainties.²⁰ Hence, the *reliable* results of the London model are only those that are insensitive to the cutoff chosen. Still, one can fit the data $h(\mathbf{r})$ to a properly truncated sum (29) and extract the best-fit parameters λ_L and ξ along with their H dependence. Interestingly enough, the so extracted $\xi(H)$ behaves as a function of H in nearly the same manner as $\rho_c(H)$ extracted directly from the field distribution; it is found for a few materials that in high fields $\rho_c \approx \xi + C$ with a material dependent constant C .¹

We now consider the data on $\rho_c(H)$ for V_3Si , $NbSe_2$, YNi_2B_2C , and $CeRu_2$ provided in Refs. 18 and 21–23, respectively, and summed up in the review by Sonier.¹ All the samples are high-quality single crystals and have large GL parameters κ ; we assume them to be clean (the available scattering parameters are $\lambda(V_3Si) \approx 0.13$ and $\lambda(NbSe_2) \approx 0.15$). The reduced temperatures of the μ SR experiments were low: ≈ 0.22 , 0.33 , 0.19 , and 0.3 , respectively. For each material we have taken the H_{c2} at a corresponding temperature, calculated ξ_{c2} , and normalized the experimental core radius to this value to obtain $\rho_c^* = \rho_c / \xi_{c2}$. The results are plotted in Fig. 2(a) together with the theoretical ξ^* versus reduced fields $h = H / H_{c2}$. For reasons explained above we took only the data points for $h > 0.15$. We expect the experimental $\rho_c^*(h)$ and the theoretical $\xi^*(h)$ to be shifted by a material-, temperature-, and purity-dependent constant: $\xi^*(h) \approx \rho_c^*(h) + C(\lambda, T)$. Since the temperatures and impurity parameters in different experiments were different, we do not expect these shifts to be the same for the materials examined. In this situation, we have chosen the constants C so as to shift the data points as close as possible to our curve of $\xi^*(h)$. The result is shown in Fig. 2(b); the shifts needed are shown in the panel legend. Although the shifts vary, the data for different materials land nicely in a vicinity of our curve. This supports our guess of universality, a considerable ambiguity of the procedure notwithstanding.

An interesting feature of the data and of the universal curve $\xi^*(1/\sqrt{h})$ is seen in Fig. 2(c). The slope of this curve starting with the value (28) of ≈ 0.2 at $h=1$, increases to about 0.4 in the domain $0.25 < h < 0.5$ and then drops back to about 0.2 near $h \approx 0.15$. In other words, the slope does not

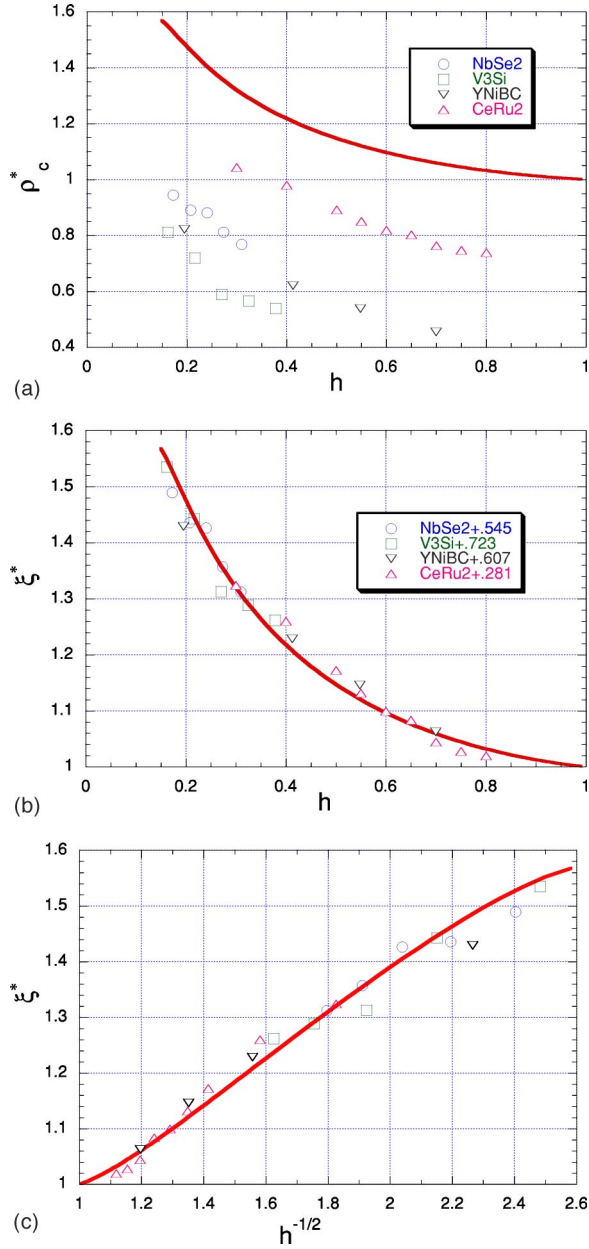


FIG. 2. (Color online) (a) the experimental core radius ρ_c normalized on $\xi_{c2} = \sqrt{\phi_0/2\pi H_{c2}(T)}$ of each compound for materials indicated in the legend; T is the temperature of each experiment. The solid line is the theoretical $\xi^*(h)$ with $h=H/H_{c2}(T)$, the same curve as in Fig. 1. (b) the same data shifted by amounts indicated in the legend. (c) the same as (b), but plotted vs $1/\sqrt{h}$.

change much in each of these broad domains,

$$\frac{d\xi^*}{d(1/\sqrt{h})} \approx 0.2 - 0.4, \quad (30)$$

or in common units,

$$\frac{d\xi}{d(1/\sqrt{H})} \approx (0.2 - 0.4) \sqrt{\frac{\phi_0}{2\pi}}. \quad (31)$$

Since the measured core size ρ_c differs from our ξ by a constant shift, we may rewrite the last estimate as

$$\frac{d\rho_c}{d(1/\sqrt{H})} \approx (115 - 230) \text{ \AA} \sqrt{kOe} \quad (32)$$

in units employed in experiments. Given our suggestion of universality, we expect the high-field slope $d\rho_c/d(1/\sqrt{H})$ for all materials to be in this range. For the set of materials discussed here, this is the case: we roughly estimate the slope as 220 for V₃Si, 190 for NbSe₂, 240 for YNi₂B₂C, and 170 $\text{\AA}\sqrt{kOe}$ for CeRu₂. The ability of our approach to provide the slope values in a good agreement with the data indicates that the model correctly catches the physics of the field dependence of the core size. The slopes are relevant in particular, given an uncertain relationship between ξ we calculate and the experimental ρ_c [uncertain shifts C in $\xi^*(h) \approx \rho_c^*(h) + C(\lambda, T)$ shown in Fig. 2(c)].

We add to this that our numerical calculations show that, in qualitative agreement with existing data on ρ_c , ξ for clean materials ($\lambda < 1$) reaches H -independent plateaus in decreasing fields.¹ The values of ξ at these plateaus decreases with scattering and with temperature. Unfortunately, the data available are still scarce and the issue of plateaus calls for more experimental and theoretical work.

A number of questions still remains to be addressed. Theoretically, it is not clear whether or not our clean limit results are compatible with the prediction of Pesh and Kramer that the core size of an isolated vortex defined as $\rho_1 = \Delta / (\partial\Delta/\partial r)_{r \rightarrow 0}$ goes to zero as $T \rightarrow 0$.²⁴ We note, however, that our results for ρ_c are meaningful only in large fields and for large GL parameters κ , whereas these authors have considered an isolated vortex in a material with $\kappa = 0.9$. The same can be said with respect to calculations of Ichioka *et al.* done for the d -wave symmetry who find a shrinking core size in decreasing temperatures.²⁵

Calculations of Miranović *et al.*⁸ of the low-temperature field dependence of the length $\rho_1 = \Delta_m / (\partial\Delta/\partial r)_{r \rightarrow 0}$ in the mixed state (Δ_m is the order-parameter maximum along the nearest-neighbor direction) show that for clean materials with $\lambda < 1$ the length $\rho_1(H)$ goes through a minimum and increases approaching H_{c2} . It also shows a much stronger field dependence on the dirty side ($\lambda > 1$) than our $\xi(H)$. A way out of this difficulty, in our opinion, is to conclude that $\rho_1(H)$ is not proportional either to our $\xi(H)$ or to existing data on the core size $\rho_c(H)$ in clean materials for which the minimum in $\rho_c(H)$ had not been recorded.¹

There is indirect experimental evidence that the scattering suppresses the field dependence of the core size. Nohara *et al.*²² report that the H dependence of ρ_c extracted from the field dependence of the specific heat coefficient γ_e and well pronounced in pure NbSe₂, in fact, disappears after doping the crystal with Ta. The doping changes the impurity parameter from 0.19 to 1.25 so that the observation is consistent with our conclusion. The data of this group on YNi₂B₂C and Y(Ni_{0.8}Pt_{0.2})B₂C are more convincing yet: the first crystal has the impurity parameter $\lambda \approx 0.4$ (i.e., it is on the clean side) whereas the Pt-doped crystal is on the dirty side with $\lambda \approx 2.4$; the H dependence of ρ_c in the doped crystal is practically absent. Still, the question of $\rho_c(H)$ in the presence of impurities could be resolved if the μ SR data were taken on a

set of the same crystals with varying mean-free path; candidates for such a study could be (e.g., crystals of $\text{LuNi}_2\text{B}_2\text{C}$ doped with Co).²⁶

We reiterate in conclusion that experimental core sizes ρ_c follow (within material- and experiment-dependent constant) the field dependence of the coherence length ξ calculated with the help of the weak-coupling BCS theory. The H dependence of ξ is pronounced at low temperatures of clean materials and becomes weaker with increasing scattering and temperature; ρ_c should do the same. We have shown that in high fields and low T 's the slopes $d\rho_c/d(H^{-1/2})$ is nearly independent of the Fermi surface shape; the theory provides an estimate of these slopes confirmed by comparison to data for a number of different high- κ materials.

ACKNOWLEDGMENTS

We are glad to thank J. Sonier for informative discussions and for providing a table of published data. Thoughtful comments of P. Miranović are greatly appreciated. Ames Laboratory is operated for the U. S. Department of Energy by Iowa State University under Contract No. W-7405-Eng-82. This work was supported by the Office of Basic Energy Sciences.

APPENDIX A

The sum (18) over m, n can be replaced with the sum over m from 0 to $\mu = m+n$ and the sum over μ from 0 to ∞ ; the former can be written as a hypergeometric function

$$S = \sum_{\mu=0}^{\infty} (2\mu-1)!! \left(-\frac{u}{2}\right)^{\mu} {}_2F_1(-\mu, 1-\sigma; 1; 2). \quad (\text{A1})$$

We now use the integral representation

$${}_2F_1(a, b; c; z) = \frac{e^{-i\pi b} z^{1-c}}{4\pi^2} \Gamma(c) \Gamma(1+b-c) \Gamma(1-b) \times \oint dt (t-z)^{c-b-1} t^{b-1} (1-t)^{-a}, \quad (\text{A2})$$

where the contour circles the branch points at $t=0$ and $t=z$ twice in opposite directions; the representation holds everywhere except points where the Γ factors diverge.²⁷ This yield

$$S = \frac{e^{i\pi(\sigma-1)}}{4\pi^2} \Gamma(1-\sigma) \Gamma(\sigma) \oint (t-2)^{\sigma-1} t^{-\sigma} \times \sum_{\mu=0}^{\infty} (2\mu-1)!! \left[-\frac{u}{2}(1-t)\right]^{\mu} dt. \quad (\text{A3})$$

The sum here (sometimes called Euler or Borel summable, see, e.g., Ref. 28) is transformed into an integral with the help of identity

$$\sum_{\mu=0}^{\infty} (2\mu-1)!! (-x)^{\mu} = \frac{2}{\sqrt{\pi}} \text{Re} \int_0^{\infty} \frac{dse^{-s^2}}{1+2s^2x}, \quad (\text{A4})$$

which is proven by formally expanding $1/(1+2s^2x)$ in powers of $2s^2x$ and integrating over s .

Then the contour integral emerges of the form

$$J = \oint (t-2)^{\sigma-1} t^{-\sigma} \frac{dt}{1+s^2u(1-t)}, \quad (\text{A5})$$

which can be transformed back to the hypergeometric form after the substitution $t=v(1+s^2u)/s^2u=vz$

$$J = \frac{4\pi^2 e^{i\pi(1-\sigma)}}{\Gamma(1-\sigma)\Gamma(\sigma)} {}_2F_1(1, 1-\sigma; 1; 2/z). \quad (\text{A6})$$

Furthermore, ${}_2F_1(1, 1-\sigma; 1; 2/z) = (1-2/z)^{\sigma-1}$ and we obtain Eq. (19) of the main text.

APPENDIX B

One has to evaluate the integral at the right-hand side of Eq. (22). We start with the Fermi cylinder

$$\int_0^{\omega_D} \frac{d\omega}{\omega} S = \frac{2}{\sqrt{\pi}} \text{Re} \int_0^{\infty} ds e^{-s^2} \int_0^{\omega_D} \frac{d\omega}{\omega} \eta(\sigma, \omega), \quad (\text{B1})$$

with

$$\eta = \frac{(1-s^2u)^{\sigma-1}}{(1+s^2u)^{\sigma}}, \quad u = \frac{v^2 q^2}{4\omega^2}. \quad (\text{B2})$$

Substitution $x = \omega^2/\omega_D^2$ transforms the integral over ω to

$$J = \frac{1}{2} \int_0^1 dx \frac{(x-y)^{\sigma-1}}{(x+y)^{\sigma}} = \frac{(-1)^{-\sigma}(1+y)^{1-\sigma}}{4y(\sigma-1)(2y)^{-\sigma}} {}_2F_1\left(1-\sigma, 1-\sigma; 2-\sigma; \frac{1+y}{2y}\right) - \frac{(-1)^{\sigma}}{4} \left[\psi\left(\frac{1-\sigma}{2}\right) - \psi\left(1-\frac{\sigma}{2}\right) \right], \quad (\text{B3})$$

where

$$y = \frac{s^2 v^2 q^2}{4\omega_D^2} \ll 1 \quad (\text{B4})$$

because large values of s are cut off by e^{-s^2} ; even at H_{c2} of clean materials this inequality reduces to the standard BCS restriction $\hbar\omega_D \gg \Delta_0$. Utilizing the reflection formulas for the Digamma function,¹² $\psi(1-z) = \psi(z) + \pi \cot(\pi z)$, the expression in square parentheses is rewritten as

$$\psi\left(\frac{1+\sigma}{2}\right) - \psi\left(\frac{\sigma}{2}\right) - \frac{2\pi}{\sin(\pi\sigma)}. \quad (\text{B5})$$

We further use the asymptotic formula 15.3.13 of Ref. 12 for ${}_2F_1$ with $1/2y \gg 1$. Then, the real part of J assumes the form

$$\text{Re } J = -\frac{\cos(\pi\sigma)}{4} \left[\psi\left(\frac{1+\sigma}{2}\right) - \psi\left(\frac{\sigma}{2}\right) \right] - \frac{1}{2} [\ln 2 + \gamma + \psi(\sigma)] + \ln \frac{2\omega_D}{vq} - \ln s. \quad (\text{B6})$$

The integration over s in Eq. (B1) is now straightforward: the s independent part of $\text{Re } J$ enters, the result being unchanged because $(2/\sqrt{\pi}) \int_0^{\infty} dse^{-s^2} = 1$. Furthermore, $(2/\sqrt{\pi}) \int_0^{\infty} dse^{-s^2} \ln s = -\gamma/2 - \ln 2$. Collecting all terms in the

self-consistency equation (22) we obtain Eq. (23). As expected, the large parameter ω_D cancels out from the final result.

For the 3D situation, we have to replace in 2D Eq. (B1) $(2/\sqrt{\pi})\int_0^\infty ds e^{-s^2} \text{Re } J$ with $\sqrt{\pi}\int_0^\infty ds \text{erfc}(s)\text{Re } J$. As in 2D, the s -independent part of $\text{Re } J$ enters, the result being unchanged since $\sqrt{\pi}\int_0^\infty ds \text{erfc}(s)=1$, whereas $\sqrt{\pi}\int_0^\infty ds \text{erfc}(s)\ln s=-1-\gamma/2$. This gives the 3D version of Eq. (23).

APPENDIX C

An explicitly real representation of the integral (16) is given in Ref. 10 for the Fermi sphere. Here we provide it for

the 2D isotropic case of Eq. (19). To this end, one separates the integration domain in two: $0 < s < 1/\sqrt{u}$ and $1/\sqrt{u} < s < \infty$. In the first, the integration variable is changed to $y = s/\sqrt{u}$, whereas in the second to $y = (s\sqrt{u})^{-1}$. Then we obtain

$$S(u, \sigma) = \frac{2}{\sqrt{\pi u}} \int_0^1 dy \frac{(1-y^2)^{\sigma-1}}{(1+y^2)^\sigma} \times \left[\exp\left(-\frac{y^2}{u}\right) - \cos(\pi\sigma) \exp\left(-\frac{1}{y^2 u}\right) \right], \quad (\text{C1})$$

the form easy to deal with numerically.

-
- ¹J. E. Sonier, *J. Phys.: Condens. Matter* **16**, 4499 (2004).
²P. DeGennes, *Superconductivity of Metals and Alloys* (Addison-Wesley, New York, 1989).
³M. Tinkham, *Introduction to Superconductivity* (McGraw-Hill, 1996).
⁴A. A. Golubov and U. Hartmann, *Phys. Rev. Lett.* **72**, 3602 (1994).
⁵E. H. Helfand and N. R. Werthamer, *Phys. Rev.* **147**, 288 (1966).
⁶M. Ichioka, A. Hasegawa, and K. Machida, *Phys. Rev. B* **59**, 184 (1999).
⁷M. Ichioka, A. Hasegawa, and K. Machida, *Phys. Rev. B* **59**, 8902 (1999).
⁸P. Miranović, M. Ichioka, and K. Machida, *Phys. Rev. B* **70**, 104510 (2004).
⁹V. G. Kogan, *Phys. Rev. B* **32**, 139 (1985).
¹⁰V. G. Kogan and N. Nakagawa, *Phys. Rev. B* **35**, 1700 (1987). In this paper, S has been used to calculate the SN phase boundary of a thin film in parallel field. The boundary conditions employed were later questioned by P. Scotto and W. Pesh, *J. Low Temp. Phys.* **84**, 301 (1991), and by J. Hara and K. Nagai, *J. Phys. Soc. Jpn.* **63**, 2331 (1994). The integral representation of S of this paper is not related to boundary conditions and is correct.
¹¹G. Eilenberger, *Z. Phys.* **214**, 195 (1968).
¹²*Handbook of Mathematical Functions*, edited by M. Abramowitz and A. Stegun, Natl. Bur. Stand. Appl. Math. Ser. Vol. 55 (U.S. GPO, Washington, DC, 1965).
¹³L. P. Gor'kov, *Zh. Eksp. Teor. Fiz.* **37**, 833 (1959) [*Sov. Phys. JETP* **10**, 593 (1960)].
¹⁴L. N. Bulaevskii, *Zh. Eksp. Teor. Fiz.* **68**, 1278 (1973) [*Sov. Phys. JETP* **38**, 634 (1974)].
¹⁵The same result can be shown to hold for a Fermi surface consisting of two sheets, a sphere, and a cylinder with two different but constant gaps; the derivation will be published elsewhere.
This model Fermi surface is proven to work well for MgB₂; see, e.g., V. G. Kogan, *Phys. Rev. B* **66**, 020509(R) (2002) and P. Miranović, K. Machida, and V. G. Kogan, *J. Phys. Soc. Jpn.* **72** (2), 221 (2003). The model is probably good for NbSe₂ as well.
¹⁶A. A. Abrikosov, *Fundamentals of the Theory of Metals* (North-Holland, New York, 1988).
¹⁷The function $\xi^*(h)$ for $h < 0.15$ oscillates with decreasing amplitude when $h \rightarrow 0$ where $\xi^* \rightarrow e^{\gamma/2} \approx 1.33$. Formally, the oscillations are due to the branch point of the integrands (16) and (19), which produces $\cos(\pi\sigma)$ in the real part of the integral. The physical significance of this zero- T clean limit behavior is unclear.
¹⁸J. E. Sonier, F. D. Callaghan, R. I. Miller, E. Boaknin, L. Taillefer, R. F. Kiefl, J. H. Brewer, K. F. Poon, and J. D. Brewer, *Phys. Rev. Lett.* **93**, 017002 (2004).
¹⁹A. Yaouanc, P. Dalmas de Réotier, and E. H. Brandt, *Phys. Rev. B* **55**, 11 107 (1997).
²⁰J. R. Clem, *J. Low Temp. Phys.* **18**, 427 (1975).
²¹J. E. Sonier, R. F. Kiefl, J. H. Brewer, J. Chakhalian, S. R. Dunsiger, W. A. MacFarlane, R. I. Miller, A. Wong, G. M. Luke, and J. W. Brill, *Phys. Rev. Lett.* **79**, 1742 (1997).
²²M. Nohara, M. Isshiki, F. Sakai, and H. Takagi, *J. Phys. Soc. Jpn.* **68**, 1078 (1999).
²³R. Kadono, W. Higemoto, A. Koda, K. Ohishi, T. Yokoo, J. Akimitsu, M. Hedo, Y. Inada, Y. Ōnuki, E. Yamamoto, and Y. Haga, *Phys. Rev. B* **63**, 224520 (2001).
²⁴W. Pesh and L. Kramer, *J. Low Temp. Phys.* **15**, 367 (1974).
²⁵M. Ichioka, N. Hayashi, N. Enomoto, and K. Machida, *Phys. Rev. B* **53**, 15 316 (1996).
²⁶K. O. Cheon, I. R. Fisher, V. G. Kogan, P. C. Canfield, P. Miranović, and P. L. Gammel, *Phys. Rev. B* **58**, 6463 (1998).
²⁷P. M. Morse and H. Feshbach, *Methods of Theoretical Physics* (McGraw-Hill, New York, 1953); Vol. 1, Eq. (5.3.20).
²⁸G. H. Hardy, *Divergent Series* (Clarendon, Oxford, 1949).